


Dynamics and lifetimes of resonant phonons in the quasiparticle and nonquasiparticle regimesL. Xie  and J. Q. He**Department of Physics, Southern University of Science and Technology, Shenzhen 518055, China*

(Received 27 April 2022; revised 2 November 2022; accepted 14 November 2022; published 22 November 2022)

The dynamics and lifetimes of a phonon with model resonant interactions from the quasiparticle to nonquasiparticle regime were investigated employing Green's function and the Green-Kubo method. In the weak-coupling case, the dynamics of the resonant phonon are analogous to a damped harmonic oscillator and its lifetime τ is in accordance with the standard phonon transport theory $\tau = \frac{1}{2\Gamma}$ (Γ being the imaginary part of phonon self-energy). In the strong-coupling nonquasiparticle regime, however, the resonant phonon "propagates" in a complex form of wave packets and the actual phonon lifetime τ_{GK} as determined from the Green-Kubo formula significantly deviates from the standard $\tau = \frac{1}{2\Gamma}$ relation. Taking the four-phonon resonant AgCrSe₂ and three-phonon resonant PbSe model systems as examples, the phonon nonquasiparticle dynamics and their lifetimes in real materials are further investigated by first-principle calculations. Substantial discrepancies between τ_{GK} and τ are found for the strongly resonant phonons at high-symmetrical points in both materials. Meanwhile, the lifetime τ_{GK} of the phonons that are not subjected to resonant phonon interactions almost recovers to the conventional theoretical result τ despite the non-Lorentzian spectral feature of these phonons. It is suggested that $\omega\tau_{\text{GK}}$, instead of the conventional $\omega\tau$, can be applied as a criterion to distinguish phonon quasiparticles and nonquasiparticles in addition to the phonon spectral functions.

DOI: [10.1103/PhysRevB.106.174110](https://doi.org/10.1103/PhysRevB.106.174110)**I. INTRODUCTION**

Heat transport by phonons, or lattice thermal conductivity (κ_l), is a fundamental physical property of materials. Materials with a high κ_l have important industrial applications in the thermal management of mechanical, electrical, and nuclear systems [1], while low κ_l materials have potential applications as high-efficient thermoelectrics [2], thermal barriers, and thermal insulating materials. In high κ_l materials, phonons are weakly coupled; thus, they can be viewed as ideal quasiparticles. The heat transport by these ideal phonon quasiparticles can be well described by the standard phonon Boltzmann transport equation (BTE) [3–7]. In contrast, the phonons in low κ_l materials are highly anharmonic and usually deviate from the ideal phonon quasiparticle picture. In strongly anharmonic crystals, it is suggested that the standard BTE is no longer appropriate as it is simply a kinematic approximation, which implicitly requires $\omega\tau \gg 1$ (ω : phonon frequency; τ : phonon lifetime, which is usually characterized by the full width at half maximum $1/\tau$ of the spectroscopic Lorentzian line) [4,5,8]. In fact, large discrepancies in κ_l between experiments and the standard BTE theories have been discovered in materials with low κ_l , including Tl₃VSe₄ [9], CsPbBr₃ [10], and La₂Zr₂O [11]. To amend the limitation of standard BTE theory, attempts have been made either by adding the heat conduction from the nonquasiparticle-like phonons in the framework of a two-channel model [9,11] or by considering the nondiagonal thermal contributions to κ_l [10,12,13]. However, the fundamental principles of these strategies are still

based in the standard BTE theory, which paradoxically extrapolates the weak-coupling approximation $\omega\tau \gg 1$ to strongly anharmonic crystals. Furthermore, whether τ can be unambiguously defined for certain materials from the viewpoint of spectroscopies remains in question. For example, experimental data have shown that the degenerate zone center optical phonons in CuCl [14], PbTe [15–17], and PbSe [16,18] are of non-Lorentzian shape and even split into two individual peaks due to strong anharmonicity. These phonons are usually considered nonquasiparticles. Their dynamics, as well as their phonon lifetimes, are not well understood and should be re-investigated carefully beyond the current standard BTE theory.

Here, by taking the strongly anharmonic resonant phonon as a model system, we investigate its dynamics and lifetimes in both weak-coupling quasiparticle and strong-coupling nonquasiparticle regimes using Green's function (GF) [19,20] and the Green-Kubo (GK) method [21–25]. The numerical calculations of the resonant phonon's spectral function and time-correlation function demonstrated that the dynamics of the resonant phonon were similar to a damped harmonic oscillator (DHO) in the limit of weak anharmonicity. With increasing phonon interactions, its spectral functions are characterized by non-Lorentzian and nonquasiparticle shape features, while its time-correlation functions considerably differ from those of DHOs and show unusual nonlinear oscillations. Using the Green-Kubo formula, we obtain the phonon lifetime unambiguously and self-consistently in both the quasiparticle and nonquasiparticle regime. In the quasiparticle regime, the resonant phonon lifetime, as calculated by the GK method τ_{GK} , approached the values predicted by standard theory. In the nonquasiparticle regime, however, τ_{GK} decreased much slowly with increasing phonon interactions

*Corresponding author: he.jq@sustech.edu.cn

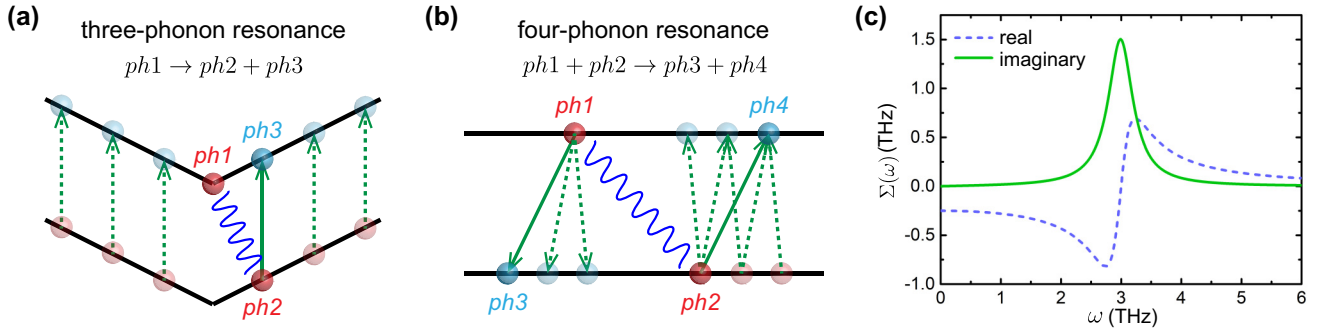


FIG. 1. Schematic diagrams of the phonon dispersion for (a) three phonon resonance and (b) four phonon resonance. (c) The real part and imaginary part of phonon self-energy calculated with $\omega_0 = 3$ THz, $\gamma_0 = 0.5$ THz, $A = 10^{-5}$ THz³ K⁻², and $n = 2$ at $T = 474.3$ K for the resonant phonon interactions [Eqs. (6) and (7)].

and reached saturation, leading to a large gap between τ_{GK} and that according to the standard phonon transport theories. These results are also demonstrated for the resonant phonons in the real materials AgCrSe₂ and PbSe by first-principle calculations and many-body perturbation theories, which highlights the universality of the Green-Kubo formula for phonon nonquasiparticles due to strong phonon-phonon interactions.

II. THEORY

Phonon resonance can give rise to extremely strong phonon interactions [26] and leads to low κ_l in PbTe [15,17], PbSe [16,18], AgCrSe₂ [27], and halide perovskites [28]. Figures 1(a) and 1(b) are schematics of the two most common types of resonant phonon interactions, i.e., three-phonon and four-phonon resonances in crystals. The black solid lines in Figs. 1(a) and 1(b) are indications of the phonon dispersions that facilitate resonant phonon interactions while conserving both momentum and energy. For the three-phonon resonance process shown in Fig. 1(a), the acoustic phonon branch and one of the optical phonon branches have similar dispersion patterns and are parallel to each other. In this case, the phonon on the upper optical phonon dispersion at zone center (ph1) can easily excite any phonon on the lower acoustic phonon dispersion (ph2), creating a new optical phonon on the upper optical phonon branch (ph3) as $\text{ph1} + \text{ph2} \rightarrow \text{ph3}$. As a consequence, the scattering phase space for the zone center phonon ph1 is huge, and theoretically ph1 resonantly interacts with other phonons. Three-phonon resonance was proposed to explain the unusual non-degenerate behaviors of the zone center optical phonons in CuCl by Kanellis *et al.* [14]. Similarly, the four-phonon resonance originates from the phonons lying on two flat phonon branches. For example, the phonon on one of the flat phonon branches (ph1) can readily combine any phonon on these two phonon branches (ph2) and yield two new phonons (ph3 and ph4, which are still on the flat phonon branches). Thus, $\text{ph1} + \text{ph2} \rightarrow \text{ph3} + \text{ph4}$, as long as the momentum and energy are conserved. It is obvious that the scattering phase space for ph1 is very dense and ph1 becomes resonant as well. In a recent study, the four-phonon resonance was used to explain the exceptionally low κ_l of AgCrSe₂ [27].

Next, we focused on the dynamics of the phonon due to resonant interactions by directly calculating the phonon

spectral function and single-particle correlation function. The spectral function $S(\omega, T)$ of a phonon at temperature T can be defined by the imaginary part of its one-particle Green's function $G(\omega, T)$ using Eq. (1) [19,20],

$$S(\omega, T) = -2\text{Im}G(\omega, T). \quad (1)$$

For a phonon with eigenfrequency ω_0 subjected to phonon-phonon interactions, $G(\omega, T)$ can be explicitly obtained from the Dyson equation as

$$G(\omega, T) = \frac{\omega_0}{\pi} \frac{1}{\omega^2 - \omega_0^2 - 2\omega_0 \Sigma(\omega, T)}, \quad (2)$$

where $\Sigma(\omega, T)$ is the phonon self-energy and can be further written by its real part $\Delta(\omega, T)$ and imaginary part $\Gamma(\omega, T)$ as $\Sigma(\omega, T) = \Delta(\omega, T) - i\Gamma(\omega, T)$. In general, $\Gamma(\omega, T)$ determines the finite phonon lifetime $\tau = [2\Gamma(\omega_0, T)]^{-1}$ in the standard phonon transport theories [29], while $\Delta(\omega, T)$ leads to the renormalization of the phonon frequency due to phonon-phonon interactions. Inserting Eq. (2) and expression of $\Sigma(\omega, T)$ into Eq. (1), we obtain Eq. (3) [19]

$$S(\omega, T) = \frac{4\omega_0^2}{\pi} \frac{\Gamma(\omega, T)}{[\omega^2 - \omega_0^2 - 2\omega_0 \Delta(\omega, T)]^2 + 4\omega_0^2 \Gamma^2(\omega, T)}. \quad (3)$$

It is worth noting that Eq. (3) is analogous to a classical DHO in its form, which is [30]

$$S_{\text{DHO}}(\omega, T) = \frac{2\omega_0}{\pi} \frac{\omega\gamma(T)}{(\omega^2 - \omega_0^2)^2 + \omega^2\gamma^2(T)}, \quad (4)$$

where $\gamma(T)$ is the damping parameter of the DHO as a function of temperature. Here, we did not distinguish the eigenfrequencies of phonons and DHOs, and the same symbol ω_0 was used throughout the text. Interestingly, Eq. (3) exactly recovers to Eq. (4) if $\Gamma(\omega, T) = \frac{\omega\gamma(T)}{2\omega_0}$ and the phonon frequency shift is neglected [$\Delta(\omega, T) \approx 0$]. This simple approximation directly links the damping parameter of DHOs to the phonon lifetime as $\tau(T) = [2\Gamma(\omega_0, T)]^{-1} = \gamma(T)^{-1}$. In fact, Eq. (4) has been widely applied in Raman, inelastic neutron, and x-ray spectroscopies [31] as a fitting function to extract the lifetime information of phonons. In addition to the frequency domain, the phonon dynamics can also be studied in the time domain via single-particle correlation function

$F(t-t', T)$ [20], which is related to $S(\omega, T)$ as

$$F(t-t', T) = \int_{-\infty}^{+\infty} \frac{1}{e^{\beta\hbar\omega} - 1} S(\omega, T) e^{-i\omega(t-t')} d\omega, \quad (5)$$

where $\beta^{-1} = k_B T$, and k_B is the Boltzmann constant.

Given Eqs. (3) and (5), the phonon dynamics of a resonant phonon can be readily obtained as long as the resonant phonon interactions $\Sigma(\omega, T)$ are known. Unfortunately, the analytical forms of three-phonon and four-phonon resonance are still unclear despite their straightforward physical pictures. For the sake of simplicity, we adopted the following form proposed for resonant scatterings, or resonant phonon-phonon interaction [32]:

$$\Gamma(\omega, T) = \frac{A\gamma_0\omega T^n}{(\omega^2 - \omega_0^2)^2 + \gamma_0^2\omega^2}, \quad (6)$$

where γ_0 is the ‘‘damping’’ constant and A is a parameter that characterizes the overall strength of phonon interactions. The temperature effect is taken into consideration by a simple power law $\Gamma(\omega, T) \sim T^n$, where n is determined by specific mechanisms of phonon interactions. For instance, three-phonon resonant interactions usually lead to $n = 1$ [33,34], while four-phonon interactions give rise to $n = 2$ [35,36]. The real part of the phonon self-energy can be evaluated from Eq. (6) via the Kramers-Kronig relationship as follows:

$$\Delta(\omega, T) = \frac{A(\omega^2 - \omega_0^2)T^n}{(\omega^2 - \omega_0^2)^2 + \gamma_0^2\omega^2}. \quad (7)$$

Figure 1(c) displays Eqs. (6) and (7) calculated with $\omega_0 = 3$ THz, $\gamma_0 = 0.5$ THz, $A = 10^{-5}$, and $n = 2$ at $T = 474.3$ K.

III. RESULTS AND DISCUSSION

In this section, we first study the phonon dynamics of the model resonant phonon interacting system and compare the phonon lifetimes calculated by Green-Kubo method to the conventional theory. Then the phonons in two model systems AgCrSe₂ and PbSe, which are characterized by strong four-phonon resonant interactions and three-phonon resonant interactions, are further investigated and discussed.

A. Model phonon resonant interacting system

The spectral functions and time-correlation functions of a phonon subjected to a model resonant phonon-phonon interaction [Eq. (6)] at different temperatures are studied with parameters $\omega_0 = 3$ THz, $\gamma_0 = 0.5$ THz, $A = 10^{-5}$, and $n = 2$. As a comparison, the dynamics for a classical DHO [Eq. (4)] under the same strength of phonon interactions, i.e., $\gamma(T) \equiv 2\Gamma(\omega_0, T)$, was also calculated. Figure 2 summarizes the spectral functions and time-correlation functions at $T = 100, 300, 474.3,$ and 600 K, as calculated by the DHO model (black curves) and GF (red curves), respectively. These temperatures were chosen specifically to generate nominal $\omega_0\tau(T)$ values of 22.5, 2.5, 1, and 0.62, which cover the phonon interactions from the weak- to extremely strong-coupling regions. In the weak-coupling region [$\omega_0\tau(T) = 22.5$, $T = 100$ K], the spectral functions $S(\omega, T)$ predicted by the DHO model and GF were similar to each other in their single-peak

Lorentzian-like line shape. Here, the phonon is considered a quasiparticle, as it has well-defined energy and linewidth (or lifetime). In addition, the corresponding time-correlation functions $F(t-t', T)$ ($t' = 0$) were well-defined oscillations. Indeed, it has been proved that the long-time behavior of the correlation function $F(t-t', T)$ would reduce to the well-known form $\exp(-\gamma t)\cos(\omega_0 t)$ when $\omega_0\tau(T) \gg 1$ [37].

In the mild- to extremely strong-coupling region, however, the phonon dynamics according to the DHO model and GF are drastically different in both frequency and time domains. Notably, all the spectral functions for the classical DHO model were still of single peak shape with increasing phonon interactions. Above the critical temperature $T = 474.3$ K [$\omega_0\tau(T) = 1$], the phonon spectral function flattened and almost vanished, which is typically considered a hallmark of the breakdown of the phonon quasiparticle picture. Moreover, the corresponding time-correlation function $F(t-t', T)$ ($t' = 0$) decayed rapidly and dropped to zero within ~ 1 ps when $\omega_0\tau(T) \leq 1$. These results are trivial and have been reported previously in the literature. In comparison, the spectral functions according to GF were no longer of single peak shape, but split into two peaks with increasing resonant phonon interactions. This splitting of the phonon spectral function agrees with the experimental observation in CuCl [14], PbTe [15,17], and PbSe [18]. This characteristic non-Lorentzian two-peak feature in the phonon spectrum also departs from the phonon quasiparticle picture, since the energies and linewidths cannot be consistently defined spectroscopically in any sense. Furthermore, the quasiparticle picture even failed when $\omega_0\tau(T) = 2.5 > 1$ at 200 K, while a single well-defined peak was found for the DHO model. As a result, we questioned whether $\omega_0\tau(T)$ is an appropriate or quantitatively accurate criterion for the validity of phonon quasiparticle approximations in materials with strong anharmonicity.

In the time domain, the time-correlation functions $F(t-t', T)$ ($t' = 0$) calculated by GF were dramatically different from their DHO counterparts as well. Unlike those of DHOs, the time-correlation functions $F(t-t', T)$ according to GF consisted of several wave packets. For example, there were four clear wave packets, each lasting from 0 to ~ 1 ps, ~ 1 to ~ 2 ps, ~ 2 to ~ 3.5 ps, and ~ 3.5 to ~ 5 ps, for $\omega_0\tau(T) = 2.5$. With increasing phonon interactions, the shape of $F(t-t', T)$ became nonperiodic and much more complicated. Nonetheless, all of them showed correlations up to ~ 3 – 4 ps even for the most strong-coupling case [$\omega_0\tau(T) = 0.62$, $T = 600$ K]. These peculiar nonlinear oscillations in $F(t-t', T)$ can be phenomenologically explained by the two-peak structure of the spectral functions $S(\omega, T)$ from the perspective of Fourier transform [Eq. (5)]. Taking $\omega_0\tau(T) = 1$ as an example, the two sharp and isolated peaks in the spectral/frequency domain can be approximately considered as a superposition of two oscillators in the time domain, in which the frequency of one oscillator is smaller than ω_0 and the other is larger than ω_0 . More importantly, the ‘‘linewidths’’ of these two peaks were much smaller than that of DHO, which hence explained the weak ‘‘damping’’ in $F(t-t', T)$.

The complex oscillation that persists up to ~ 3 – 4 ps in the time-correlation function $F(t-t', T)$ indicated that the lifetime of the model resonant phonon was longer than $\tau = \frac{1}{\Gamma}$,

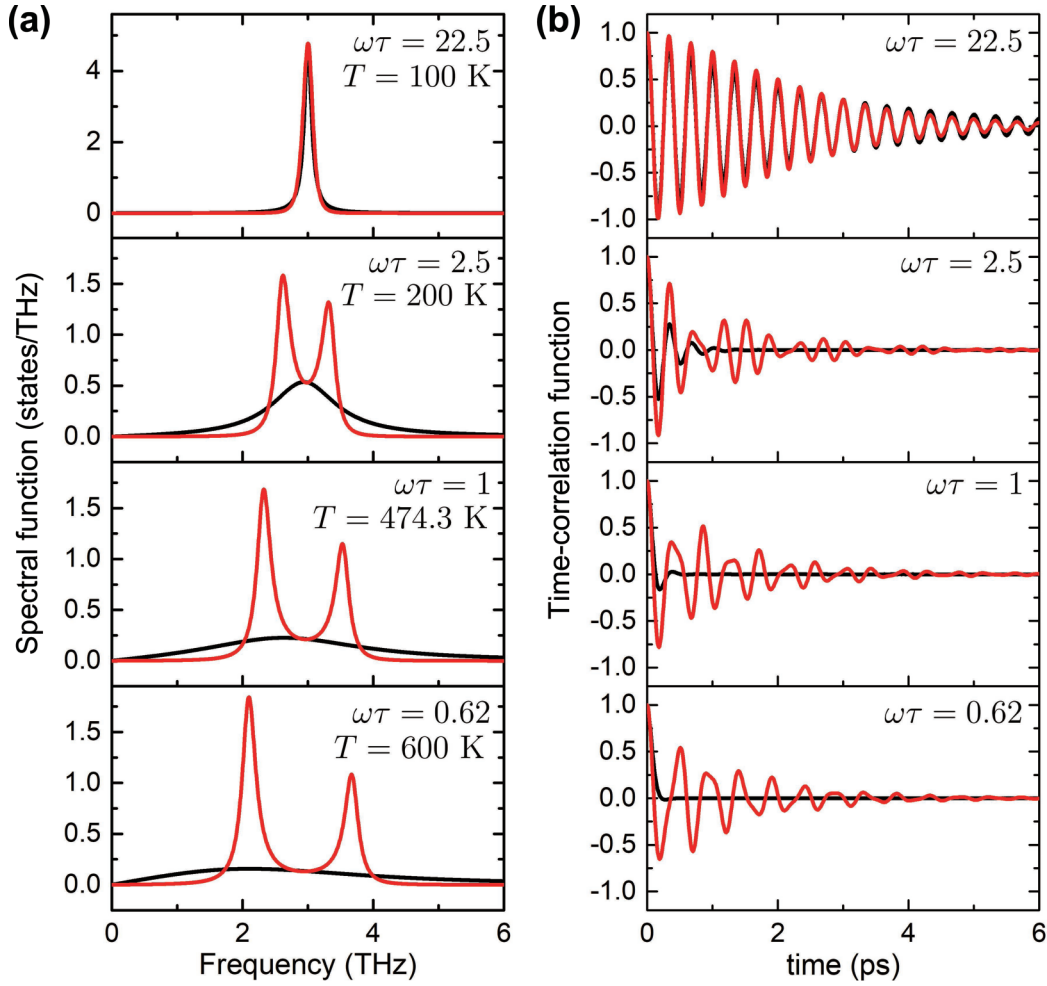


FIG. 2. (a) Spectral functions and (b) time-correlation functions of the resonant phonon [Eq. (3)] (red solid lines) and the DHO [Eq. (4)] (black solid lines) at different temperatures (or interaction strength), calculated with $\omega_0 = 3$ THz, $\gamma = 0.5$ THz, $A = 10^{-5}$ THz³ K⁻², and $n = 2$.

which was expected from the standard transport theory, especially when $\omega_0\tau(T) \leq 1$. To overcome this inconsistency, we referred to Refs. [21–25] and defined the phonon lifetime as an integration of the phonon spectral function $S(\omega, T)$, as

$$\tau_{\text{GK}}(T) \equiv \frac{\pi}{2} \int_{-\infty}^{+\infty} \frac{c_V(\omega, T)}{c_V(\omega_0, T)} S^2(\omega, T) d\omega, \quad (8)$$

where $c_V(\omega, T) = (\beta\hbar\omega)^2 \frac{k_B \exp(\beta\hbar\omega)}{[\exp(\beta\hbar\omega) - 1]^2}$ is the harmonic phonon heat capacity. Note that Eq. (8) is actually a wave formalism of phonon lifetime and its application is not limited by the shape of the phonon spectrum. In other words, we can determine the phonon lifetime from Eq. (8) unambiguously, whether $S(\omega, T)$ is characterized by single Lorentzian peak or (double) non-Lorentzian peaks (or whether phonons are quasiparticles or nonquasiparticles). In the weak-coupling limit ($\Sigma \rightarrow 0$), it can be proved that Eq. (8) would recover to the general kinematic approximation $\tau_{\text{GK}} \approx \frac{1}{2\Gamma}$ for quasiparticles [21–23]. Using Eq. (8), we calculated the lifetime for the resonant phonons by inserting Eqs. (3) and (4) for DHOs at different temperatures, or different coupling strengths. As shown in Fig. 3, the lifetime of DHOs calculated using the wave formalism $\tau_{\text{GK}}^{\text{DHO}}(T)$

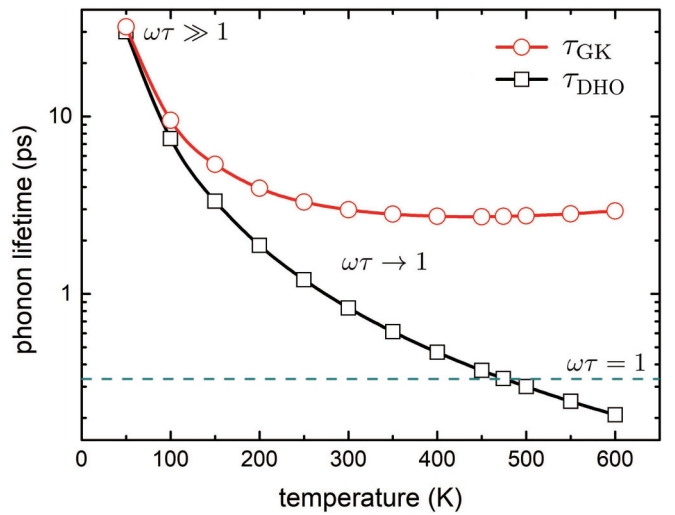


FIG. 3. Phonon lifetime τ_{GK} as a function of temperature, calculated by the Green-Kubo method [Eq. (8)] for the resonant phonon [Eq. (3)] (red circles) and the DHO [Eq. (4)] (black rectangles), respectively. The green dashed line indicates the critical phonon lifetime that leads to $\omega\tau = 1$ according to standard theory.

(black rectangles) decreased monotonically with increasing temperature (or phonon interactions). This result agrees with the typical behavior of phonon lifetime with increasing phonon interactions and temperature. Beyond the critical point $\omega\tau = 1$ (green dashed line), at which the DHO spectral function is non-Lorentzian and its lifetime is difficult to define by standard theory, we obtained the DHO lifetime according to the Green-Kubo method. In fact, the numerical integration of Eq. (4) resulted in $\tau_{\text{GK}}^{\text{DHO}}(T) = \tau = [2\Gamma(\omega_0, T)]^{-1}$ no matter the values of ω_0 , γ_0 , A , n , and T [38]. Although we are unable to give a rigorous proof here, we inferred that $\tau_{\text{GK}}^{\text{DHO}}(T)$ should be exactly equivalent to $[2\Gamma(\omega_0, T)]^{-1}$ analytically. This is a very interesting finding as it directly links the wave formalism of phonon lifetime to the standard kinematic transport theory in the special case of DHOs. That is, the conventional $\tau = \frac{1}{2\Gamma}$ for phonon lifetime is valid for both quasiparticles and nonquasiparticles when phonons are DHOs or have the unique line shape of DHOs. Thus, we can use $\tau_{\text{GK}}^{\text{DHO}} = \frac{1}{2\Gamma}$ as a reference when phonon lifetimes are compared in terms of wave formalism and the standard kinematic approximation.

In most cases, however, phonons are not ideal DHOs, and their lifetimes as a function of temperature (or phonon interactions) should deviate from the benchmark $\tau_{\text{GK}}^{\text{DHO}} = \frac{1}{2\Gamma}$. As shown in Fig. 3, the $\tau_{\text{GK}}^{\text{RP}}(T)$ calculated by Eq. (3) for the model resonant phonon (red circles) was slightly higher than the $\tau_{\text{GK}}^{\text{DHO}}(T)$ below 100 K, or in the quasiparticle regime [$\omega_0\tau(T) \gg 1$], which is consistent with the conclusion that $\tau_{\text{GK}} \rightarrow \frac{1}{2\Gamma}$ in the weak-coupling limit [21–23]. With increasing phonon interactions [$\omega_0\tau(T) \rightarrow 1$], $\tau_{\text{GK}}^{\text{RP}}(T)$ also decreased, but at a much slower rate than $\tau_{\text{GK}}^{\text{DHO}}(T)$. At 300 K, $\tau_{\text{GK}}^{\text{RP}}(T)$ was ~ 3 ps, while the reference $\tau_{\text{GK}}^{\text{DHO}}(T)$ was less than 1 ps. Such a large gap in phonon lifetime is in agreement with the significant differences in the phonon time-correlation functions [Fig. 2(b)]. Unexpectedly, $\tau_{\text{GK}}^{\text{RP}}(T)$ even stopped decreasing with further increasing temperatures and phonon interactions. Instead, it reached a plateau (~ 2.9 ps) at around 400–500 K and increased marginally at higher temperature. The increase in phonon lifetime with increasing temperature or phonon interactions is unexpected and very unusual. It can only be obtained when the full phonon spectrum contribution to the phonon lifetime is considered. This complex behavior of phonon lifetime as a function of temperature is the key result of this work and the limitation of standard $\tau = \frac{1}{2\Gamma}$ for phonon lifetime was clearly demonstrated. Therefore, the use of $\omega_0\tau_{\text{GK}}$, instead of $\omega_0\tau$, may be more accurate as a basic criterion to distinguish quasiparticles and nonquasiparticles. For example, the minimum $\omega_0\tau_{\text{GK}}$ value for the resonant phonon was ~ 9 at around 400–500 K, which is much larger than 1 and suggests quasiparticle-like phonon transports despite its peculiar nonquasiparticle-like two-peak feature. In contrast, $\omega_0\tau$ was ~ 1 in the same temperature range according to the standard phonon transport theory.

In the following two sections, the resonant phonons in real materials AgCrSe₂ and PbSe will be further discussed. These two materials are chosen specifically because the low-lying transverse acoustic (TA) phonons in AgCrSe₂ is dominated by strong four-phonon resonant interactions [27], while the transverse optical (TO) phonon in PbSe is well known to have notable three-phonon resonant interactions

[16,18]. The phonon dispersions and phonon-phonon interactions of AgCrSe₂ and PbSe were calculated in a combination of density functional theory and the temperature-dependent effective potential (TDEP) method [7]. The details of the calculation of AgCrSe₂ are reported elsewhere [27]. For PbSe, similar procedures were carried out with a plane wave energy cutoff of 450 eV and the electron configurations of Pb and Se as $5d^{10}6s^26p^2$ and $4s^24p^4$, respectively. The phonon self-energy of PbSe is calculated on a $11 \times 11 \times 11$ mesh grid. Figure 4 displays the calculated phonon dispersions of AgCrSe₂ and PbSe at 300 K. Next, we discuss the phonon spectral functions, time-correlation functions, and lifetimes of these two materials in detail.

B. Resonant phonons in AgCrSe₂

For the sake of simplicity, we focus on the low-lying TA phonons of AgCrSe₂ at the high-symmetrical F and L points and the calculated $S(\omega, T)$ [Eq. (3)] and $F(t-t', T)$ ($t' = 0$) [Eq. (5)] are given in Figs. 5 and 6. For TA1 phonons, their spectral functions are obviously far from Lorentzian shape and a clear peak splitting takes place with increasing temperature, which is qualitatively similar to those predicted by the simple resonant scattering model [Fig. 2]. It is interesting to remark that the peak positions of the spectral functions $S(\omega, T)$ deviate from the phonon eigenfrequency ω_0 ($\omega_0^{\text{TA1}} \sim 0.7\text{--}0.8$ THz) profoundly due to phonon renormalization. As a result, the time-correlation functions $F(t-t', T)$ differ from DHO-like oscillations. A notable change of oscillating frequency from 100 to 300 K can also be found for the TA1 phonons, especially the TA1 phonon at the F point (Fig. 5). For TA2 phonons, their spectral functions are in the shape of the Lorentzian function at 100 K and deviate from the conventional quasiparticle picture with the emergence of a small shoulder at higher temperatures. However, the $F(t-t', T)$ of TA2 phonons still resemble that of a DHO. In addition to the TA phonons, the LA phonons, which are barely affected by four-phonon resonant interactions, are investigated as well. As shown in Figs. 5 and 6, an accumulation of spectral density at a low frequency of ~ 1.5 THz occurs for the LA phonons. Such an unusual shift in spectral density indicates strong phonon renormalization and possible nonquasiparticle behaviors. In the time domain, the increasing spectral density at ~ 1.5 THz gives rise to the oscillation of LA phonons in the form of wave packets.

Using Eq. (8), we compare the phonon lifetimes τ_{GK} as calculated from the Green-Kubo method to that determined by the conventional theory τ . As shown in Fig. 7, the τ_{GK} of TA1 phonons (red solid circles) are about $\sim 100\%$ larger than τ (red open circles) given their strong phonon-phonon interactions and the nonquasiparticle feature in spectral functions. For TA2 phonons, the differences between their lifetimes τ_{GK} and τ are relatively smaller, but still have a sizable discrepancy of 15% at 100 K and up to 57% at 300 K. These results are consistent with our calculation results (Fig. 3) by using the simplest resonant interaction model [Eq. (6)] qualitatively. Our calculations indicate that $\omega_0\tau_{\text{GK}}$ of the TA1 phonon at the F point is already < 1 at 100 K, thus resulting in a non-negligible underestimation of phonon lifetime by the standard $\tau = (2\Gamma)^{-1}$ relation. In comparison,

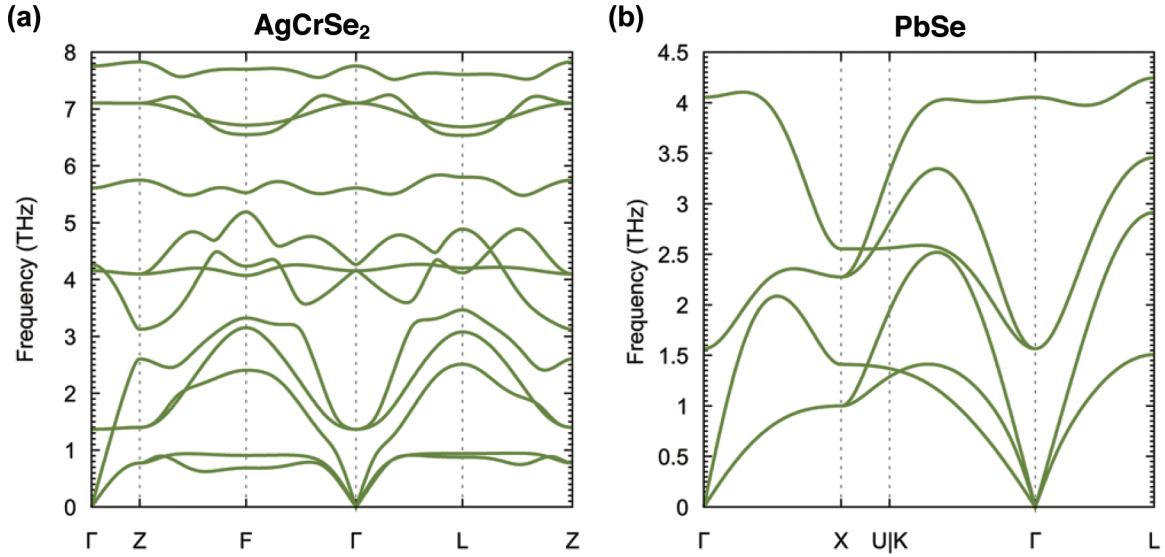


FIG. 4. Theoretical phonon dispersions of (a) AgCrSe₂ and (b) PbSe at 300 K.

the phonon lifetimes τ_{GK} of LA phonons are almost equal to τ numerically in spite of their significant nonquasiparticle spectral features. The reason is still not well understood yet and it might be partly explained by the results $\omega_0\tau_{\text{GK}} > 1$ of LA phonons. Specifically, $\omega_0\tau_{\text{GK}}$ of the LA phonon at the F (L) point decreases from 4.40 (3.07) at 100 K to 2.14 (1.55) at 300 K. Nonetheless, the good agreement between τ_{GK} and the standard theory result τ for a phonon “nonquasiparticle” does not seem like a coincidence and should deserve further studies.

C. Resonant phonons in PbSe

PbSe is another good exemplary material system that has characteristic resonant phonon interactions. Figure 8(a) displays the calculated degenerate transverse optical (TO) phonon spectral functions at the Γ point and a clear crossover from the quasiparticle regime to the nonquasiparticle regime could be found. Meanwhile, the time-correlation functions of the TO phonon follow a conventional oscillating behavior except for that at 300 K [Fig. 8(b)]. The phonon lifetime of the Γ point TO phonon is also calculated by using Eq. (8) and the

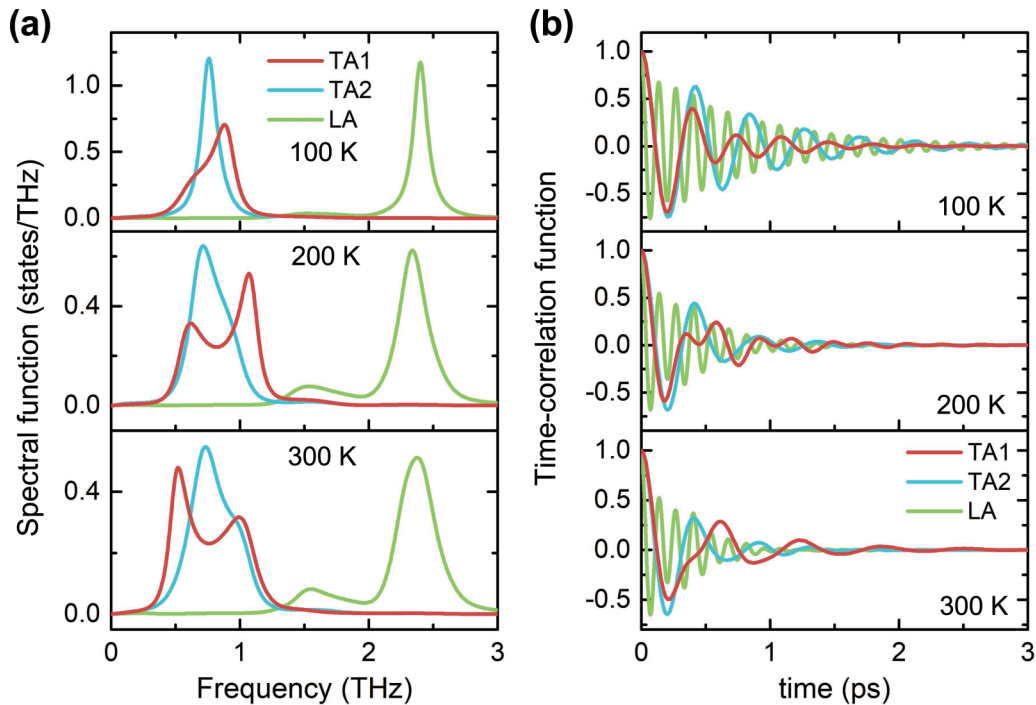


FIG. 5. (a) Spectral functions and (b) time-correlation functions of the transverse acoustic and longitudinal acoustic phonons of AgCrSe₂ at the high-symmetrical F point, calculated at 100, 200, and 300 K, respectively.

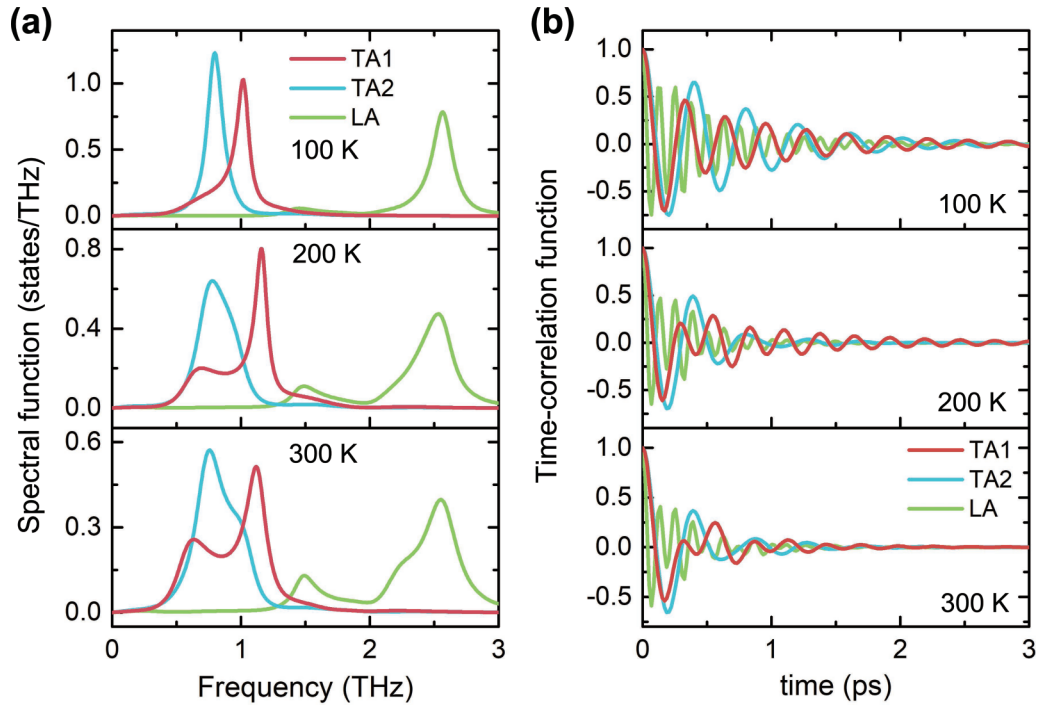


FIG. 6. (a) Spectral functions and (b) time-correlation functions of the transverse acoustic and longitudinal acoustic phonons of AgCrSe_2 at the high-symmetrical L point, calculated at 100, 200, and 300 K, respectively.

results are given in Fig. 9. The differences between τ_{GK} and τ of TO phonons are non-negligible as well, ranging from an underestimation of phonon lifetime by 12% at 100 K to over 51% at 300 K by the standard theory. The value of $\omega_0\tau_{\text{GK}}$ for

the Γ point TO phonon is ~ 1.86 at 100 K and decreases to ~ 0.84 at 300 K, which agrees with the as-observed crossover from quasiparticles to nonquasiparticles in the spectral functions. Besides the Γ point TO phonon, the spectral functions

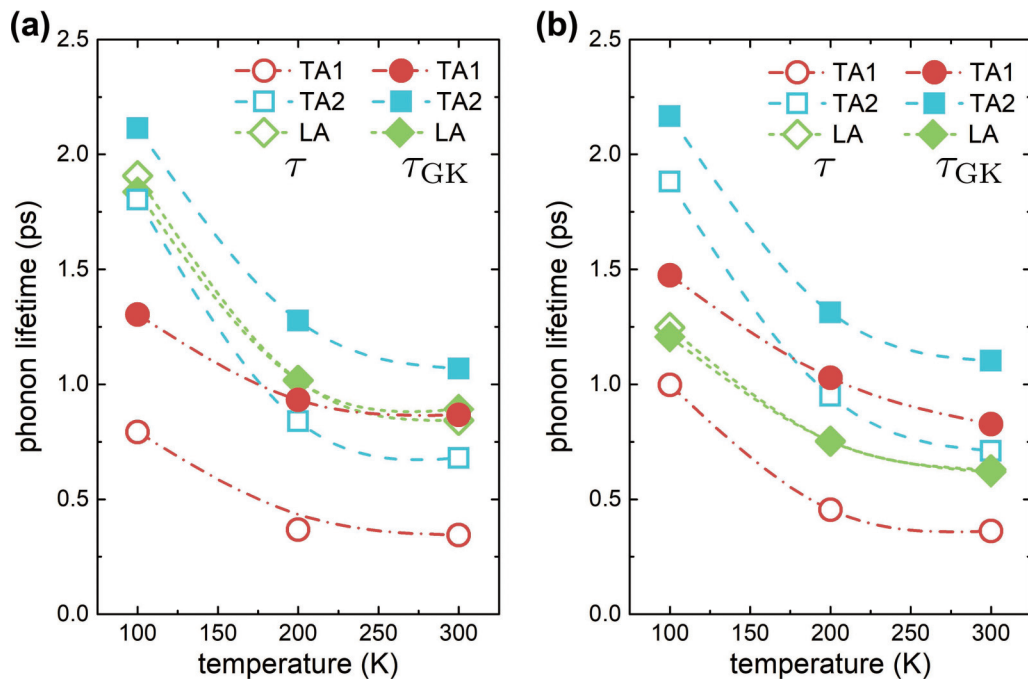


FIG. 7. Theoretical phonon lifetimes τ_{GK} (solid circles), as calculated by Green-Kubo method [Eq. (8)], and $\tau = (2\Gamma)^{-1}$ (open circles), as calculated by the standard theory, of the transverse acoustic and longitudinal acoustic phonons of AgCrSe_2 at the high-symmetrical (a) F and (b) L point at 100, 200, and 300 K. The lines are spline interpolated for better visualization.

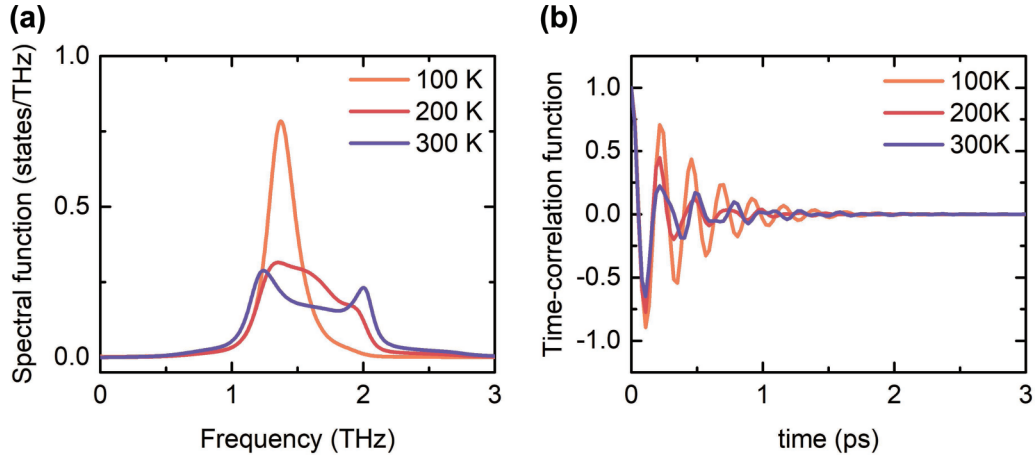


FIG. 8. (a) Spectral functions and (b) time-correlation functions of the transverse optical phonons of PbSe at the zone center Γ point, calculated at 100, 200, and 300 K, respectively.

and τ_{GK} of Γ point longitudinal optical (LO) phonons are also determined and the results are provided in Fig. S1 of the Supplemental Material [38]. An onset of spectral density at ~ 4.75 THz can be readily found in the spectral functions at 200 and 300 K, which indicates the incipient transition to nonquasiparticles. However, similar to the LA phonons in AgCrSe_2 , the calculated τ_{GK} of Γ point LO phonons match τ very well. Again, the good consistency between τ_{GK} and the standard theory τ for a phonon deviating from the conventional Lorentzian shape cannot be simply ascribed to the mild or weak coupling of phonons ($\omega_0\tau_{\text{GK}} \approx 2.67$ for the LO phonon at 300 K) and must have further implications. Careful studies in this aspect will be our future work.

IV. CONCLUSIONS

In conclusion, the dynamics and lifetimes of a simple resonant phonon and a corresponding DHO with the same

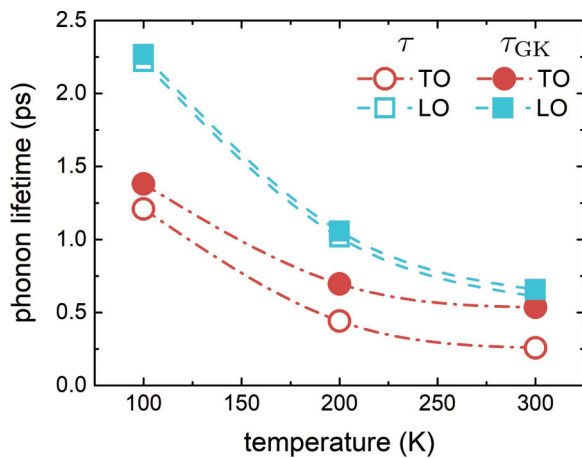


FIG. 9. Theoretical phonon lifetime τ_{GK} (solid circles), as calculated by Green-Kubo method [Eq. (8)], and $\tau = (2\Gamma)^{-1}$ (open circles), as calculated by the standard theory, of the optical phonons of PbSe at the zone center Γ point at 100, 200, and 300 K. The lines are spline interpolated for better visualization.

coupling strength using Green's function and the Green-Kubo method were studied. Our results highlight the limitation of the standard theory for phonon lifetimes ($\tau = \frac{1}{2\Gamma}$) and the necessity of a full wave formalism of phonon thermal transport, especially when the phonon spectra are characterized by non-Lorentzian and nonquasiparticle shape features. These findings are also well demonstrated in the model systems AgCrSe_2 and PbSe, which are both characterized by strong resonant phonon interactions. The huge difference in phonon lifetimes infers the mismatch between the experimental κ_l values and the theoretical BTE values is possibly a result of the neglect of the two-channel phonon heat transport [9,11] or the nondiagonal part of thermal transport [10,12], as well as the intrinsic limitation of $\tau = \frac{1}{2\Gamma}$. Using the same Green-Kubo method, it has been reported that the lifetimes of the soft phonons in GeTe are substantially larger (by a factor of 100) than those calculated by the standard method [25]. We believe our results are ubiquitous and should be readily applicable to materials with exceptionally strong anharmonicity and anomalous κ_l behaviors. These results also provide insights into the phonon dynamics of the heat transport in strong anharmonic material systems. It is suggested that a reinvestigation into the phonon spectral functions and the deviations from the standard phonon lifetime $\tau = \frac{1}{2\Gamma}$ in strongly anharmonic materials such as CuCl , PbTe , Tl_3VSe_4 , and CsPbBr_3 , is of great importance for the future development of phonon transport theories.

ACKNOWLEDGMENTS

This work was supported by the National Natural Science Foundation of China (Grants No. 51632005, No. 11874194, No. 11934007, and No. 12174176), the Natural Science Foundation of Guangdong Province (Grant No. 2015A030308001), the Leading Talents of the Guangdong Province Program (Grant No. 00201517), the Shenzhen Peacock Plan team (Grant No. KQTD2016022619565991) and the Science and Technology Innovation Committee Foundation of Shenzhen (Grant No. JCYJ20190809145205497).

- [1] D. T. Morelli and G. A. Slack, in *High Thermal Conductivity Materials*, edited by S. L. Shindé and J. S. Goela (Springer, New York, 2006), pp. 37–39.
- [2] H. J. Goldsmid, in *Introduction to Thermoelectricity* (Springer, Berlin, 2010), pp. 1–6.
- [3] R. E. Peierls, *Quantum Theory of Solids* (Clarendon, Oxford, 1955), pp. 120–121.
- [4] R. J. Hardy, *J. Math. Phys.* **7**, 1435 (1966).
- [5] G. Kirczenow, *Ann. Phys.* **125**, 1 (1980).
- [6] M. Omini and A. Sparavigna, *Phys. Rev. B* **53**, 9064 (1996).
- [7] O. Hellman, I. A. Abrikosov, and S. I. Simak, *Phys. Rev. B* **84**, 180301(R) (2011).
- [8] P. B. Allen, *Phys. Rev. B* **92**, 064106 (2015).
- [9] S. Mukhopadhyay, D. S. Parker, B. C. Sales, A. A. Puretzky, M. A. McGuire, and L. Lindsay, *Science* **360**, 1455 (2018).
- [10] M. Simoncelli, N. Marzari, and F. Mauri, *Nat. Phys.* **15**, 809 (2019).
- [11] Y. Luo, X. Yang, T. Feng, J. Wang, and X. Ruan, *Nat. Commun.* **11**, 2554 (2020).
- [12] Y. Xia, K. Pal, J. He, V. Ozoliņš, and C. Wolverton, *Phys. Rev. Lett.* **124**, 065901 (2020).
- [13] Y. Xia, V. Ozoliņš, and C. Wolverton, *Phys. Rev. Lett.* **125**, 085901 (2020).
- [14] G. Kanellis, W. Kress, and H. Bilz, *Phys. Rev. Lett.* **56**, 938 (1986).
- [15] O. Delaire, J. Ma, K. Marty, A. F. May, M. A. McGuire, M. H. Du, D. J. Singh, A. Podlesnyak, G. Ehlers, M. D. Lumsden *et al.*, *Nat. Mater.* **10**, 614 (2011).
- [16] N. Shulumba, O. Hellman, and A. J. Minnich, *Phys. Rev. B* **95**, 014302 (2017).
- [17] C. W. Li, O. Hellman, J. Ma, A. F. May, H. B. Cao, X. Chen, A. D. Christianson, G. Ehlers, D. J. Singh, B. C. Sales *et al.*, *Phys. Rev. Lett.* **112**, 175501 (2014).
- [18] M. E. Manley, O. Hellman, N. Shulumba, A. F. May, P. J. Stonaha, J. W. Lynn, V. O. Garlea, A. Alatas, R. P. Hermann, J. D. Budai *et al.*, *Nat. Commun.* **10**, 1928 (2019).
- [19] A. A. Maradudin and A. E. Fein, *Phys. Rev.* **128**, 2589 (1962).
- [20] K. N. Pathak, *Phys. Rev.* **139**, A1569 (1965).
- [21] B. Deo and S. N. Behera, *Phys. Rev.* **141**, 738 (1966).
- [22] B. S. Semwal and P. K. Sharma, *Phys. Rev. B* **5**, 3909 (1972).
- [23] U. C. Naithani, R. P. Gairola, and B. S. Semwal, *J. Phys. Soc. Jpn.* **43**, 204 (1977).
- [24] T. J. Singh and G. S. Verma, *Phys. Status Solidi B* **124**, K5 (1984).
- [25] Đ. Dangić, O. Hellman, S. Fahy, and I. Savić, *npj Comput. Mater.* **7**, 57 (2021).
- [26] T. J. Singh and G. S. Verma, *Phys. Rev. B* **25**, 4106 (1982).
- [27] L. Xie, J. H. Feng, R. Li, and J. Q. He, *Phys. Rev. Lett.* **125**, 245901 (2020).
- [28] H. Xie, S. Hao, J. Bao, T. J. Slade, G. J. Snyder, C. Wolverton, and M. G. Kanatzidis, *J. Am. Chem. Soc.* **142**, 9553 (2020).
- [29] P. Carruthers, *Rev. Mod. Phys.* **33**, 92 (1961).
- [30] H. Grabert, U. Weiss, and P. Talkner, *Z. Phys. B: Condens. Matter* **55**, 87 (1984).
- [31] B. Fåk and B. Dorner, *Phys. B (Amsterdam, Neth.)* **234-236**, 1107 (1997).
- [32] R. O. Pohl, *Phys. Rev. Lett.* **8**, 481 (1962).
- [33] D. J. Ecsedy and P. G. Klemens, *Phys. Rev. B* **15**, 5957 (1977).
- [34] M. Roufousse and P. G. Klemens, *Phys. Rev. B* **7**, 5379 (1973).
- [35] T. Feng, L. Lindsay, and X. Ruan, *Phys. Rev. B* **96**, 161201(R) (2017).
- [36] T. Feng and X. Ruan, *Phys. Rev. B* **93**, 045202 (2016).
- [37] S. K. Kim and R. S. Wilson, *Phys. Rev. A* **7**, 1396 (1973).
- [38] See Supplemental Material at <http://link.aps.org/supplemental/10.1103/PhysRevB.106.174110> for the numerical calculations of phonon lifetimes of a damped harmonic oscillator as calculated by the Green-Kubo method and the standard phonon transport theories, and for the theoretical phonon spectral functions of longitudinal optical phonons at the Γ point in PbSe.